Electronic Supporting Information

for

Metallogel Formation in Aqueous DMSO by Perfluoroalkyl Decorated Terpyridine Ligands.

Rajendhraprasad Tatikonda[a], Sandip Bhowmik[a], Kari Rissanen[a], Matti Haukka[a]* and Massimo Cametti[b]*

[1] *Department of Chemistry, Nanoscience Center, University of Jyväskylä, P.O. Box 35, 40014 Jyväskylä, Finland*

[2] *Department of Chemistry, Materials and Chemical Engineering "Giulio Natta" Politecnico di Milano, Via Mancinelli 7, 20131, Milano, Italy*

Table of contents

I. Experimental Section

2D-NMR – COSY and HMQC for Ligand 1

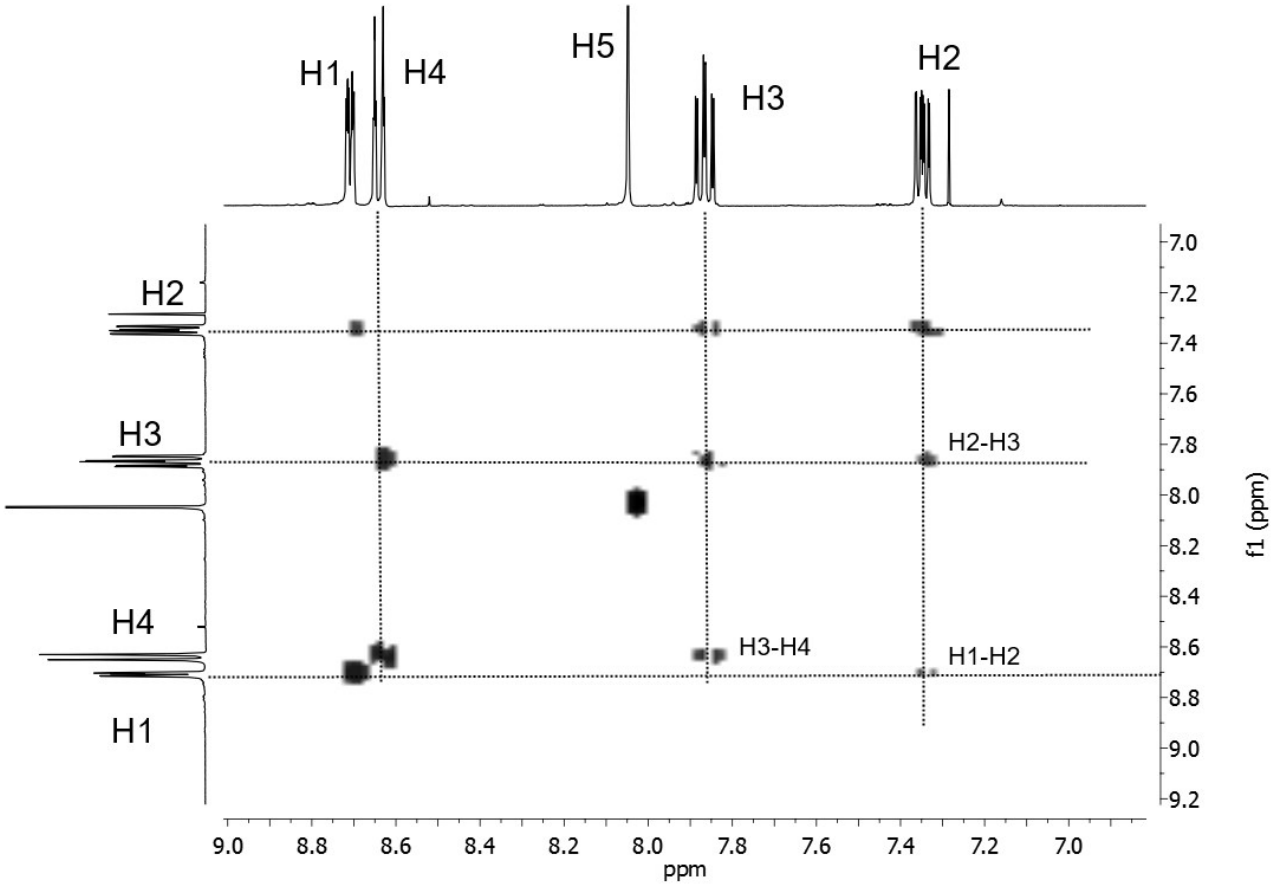

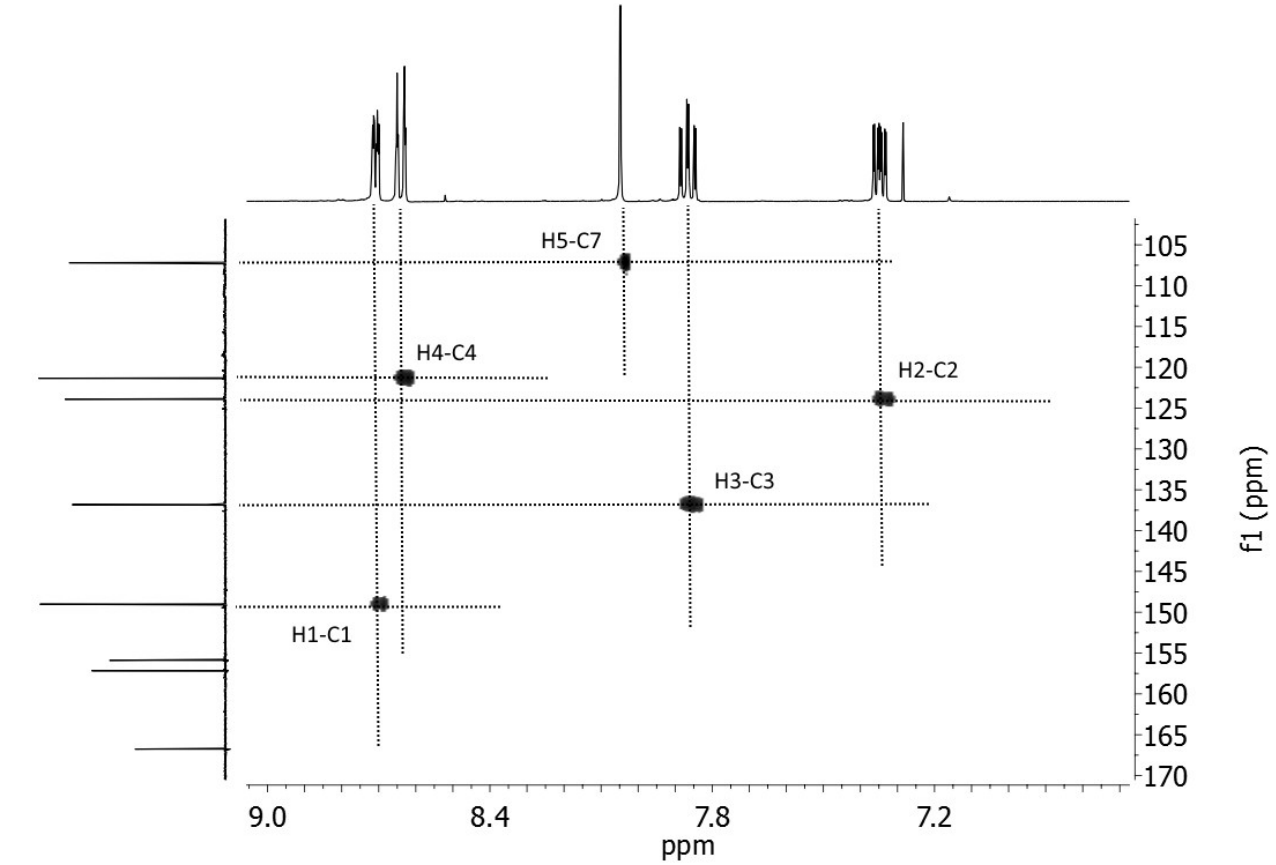

2D-NMR – COSY and HMQC for Ligand 2

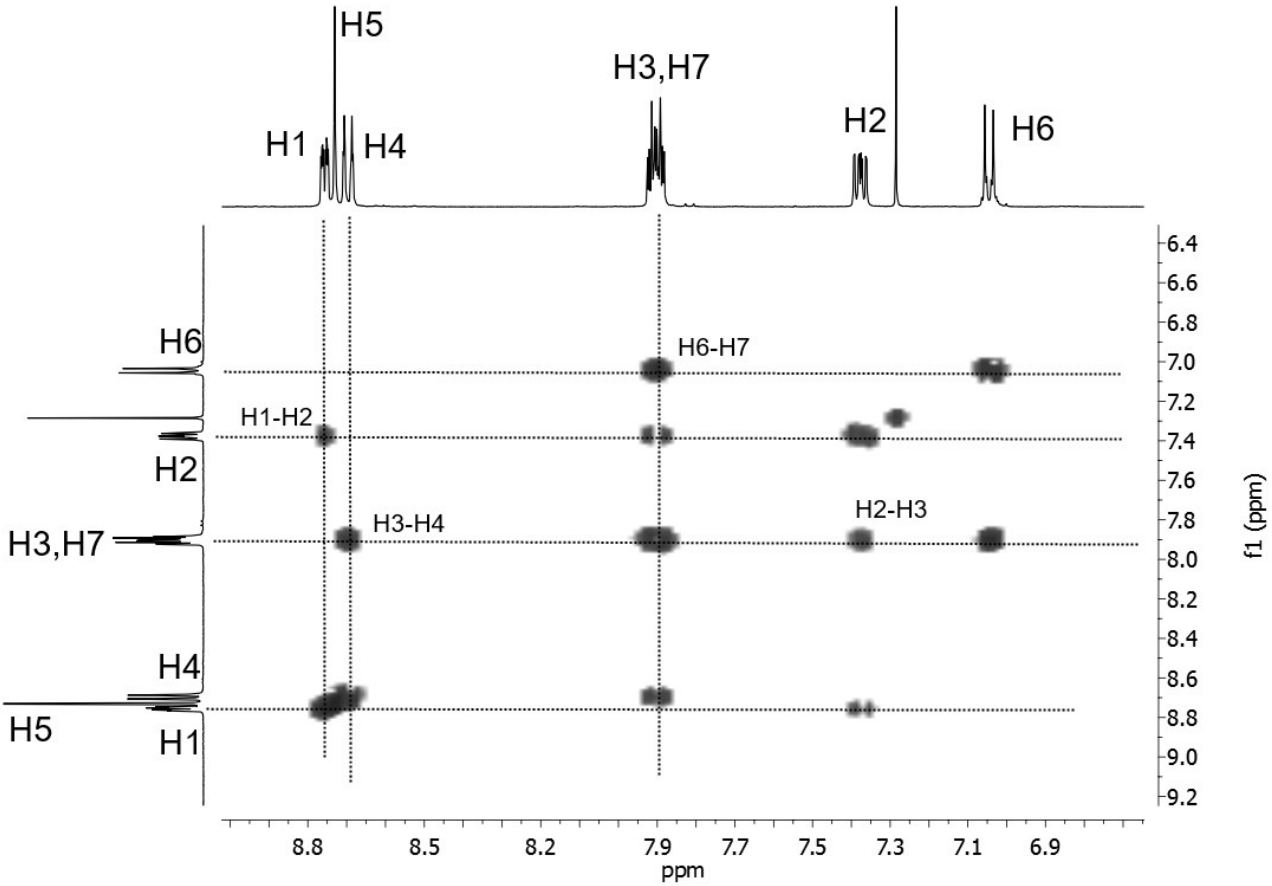

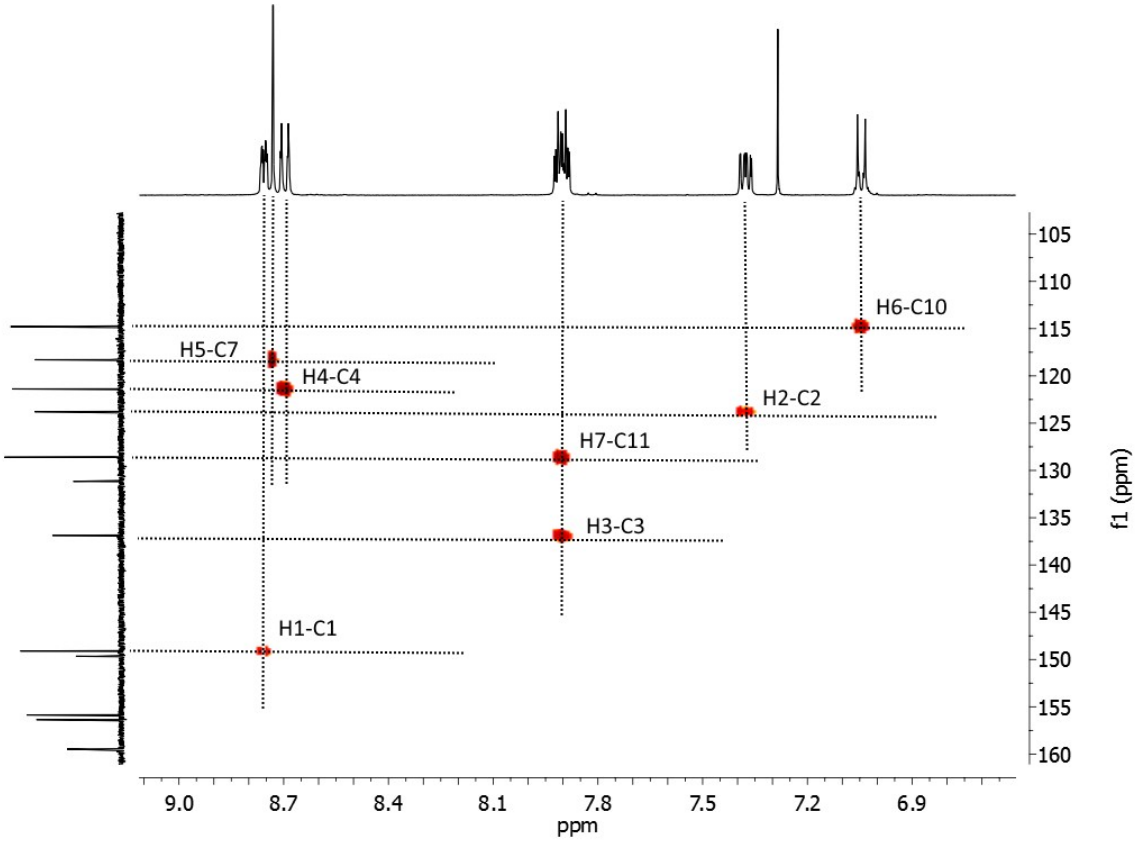

II. T_{gel} Experiments

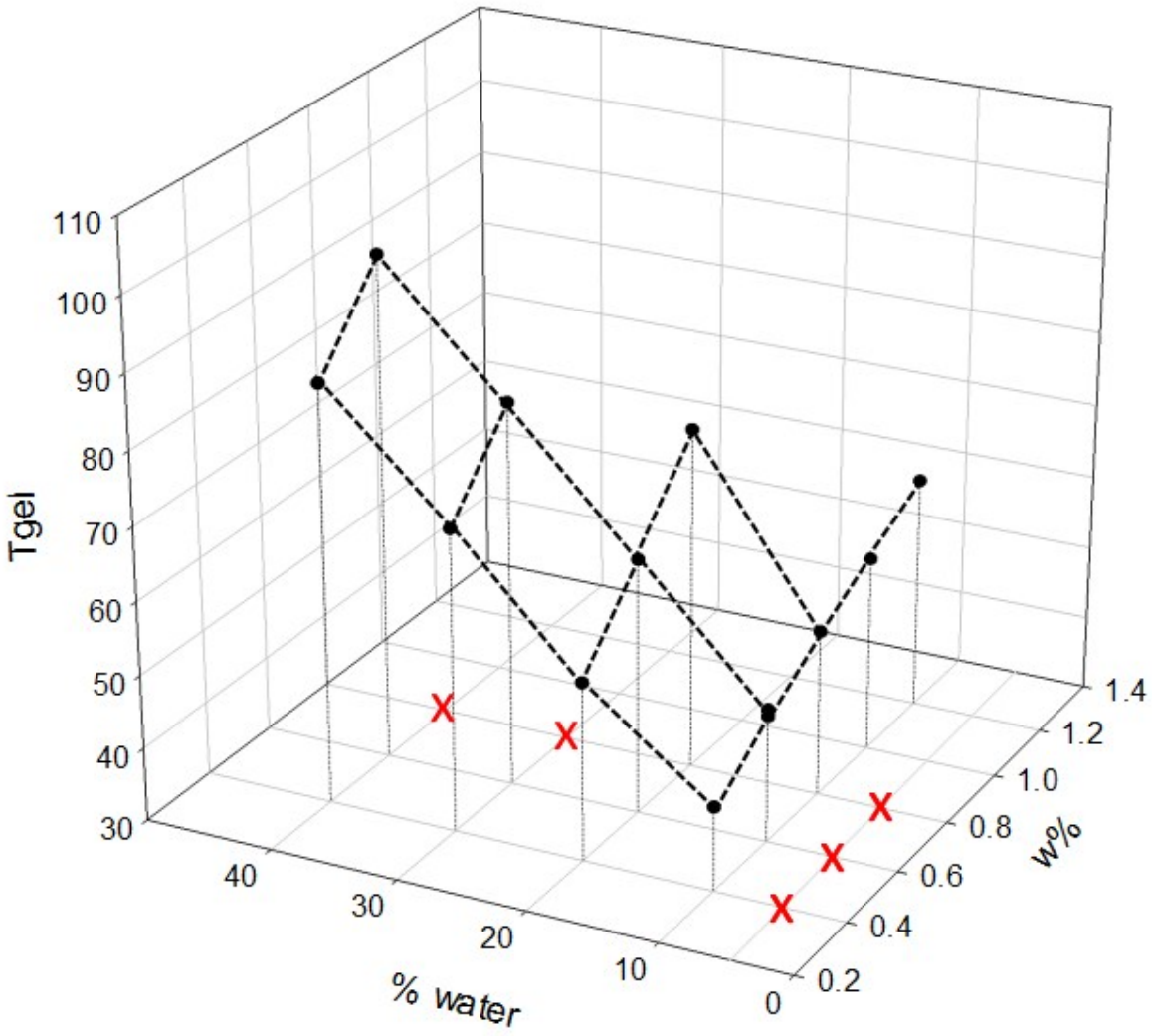

Figure S1. Graphical representation of the conditions viable to gel formation for the **2**-$FeCl_2$ system and their corresponding T_{gel}. The red cross denotes precipitation.

Tgel experiment of 1-$ZnCl_2$ gel system against the wt% in 9:1 of DMSO:Water

Conc. (w/v)	T*gel* (°C)
0.3	55.1
0.4	57.8
0.5	59.6
0.6	61.5
0.7	63.6
0.8	65.4

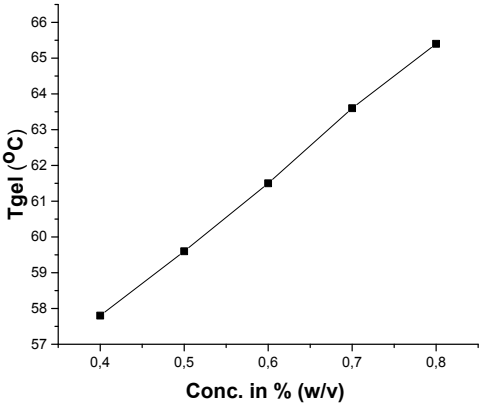

Tgel experiment of 1-$ZnCl_2$ gel system (0.6 % w/v) against the ratio of DMSO:Water.

Ratio of DMSO:Water	T*gel* (°C)
9.5:0.5	49.1
9:1	61.9
8:2	89.2
7:3	96.7
6:4	PPt

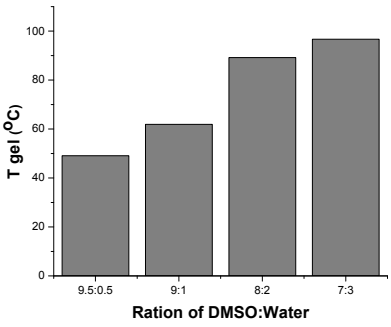

Tgel experiment of 1-$ZnCl_2$ gel system against the ratio of DMSO:Water.

(0.4 % w/v)			(0.8 % w/v)	
Ratio of DMSO:Water	T*gel* (°C)		Ratio of DMSO:Water	T*gel* (°C)
9.5:0.5	PPt		9.5:0.5	54.6
9:1	57.8		9:1	65.4
8:2	68.6		8:2	93.8
7:3	82.6		7:3	99.2
6:4	92.4		6:4	PPt

Tgel experiment of 1-$HgCl_2$ gel system against the wt% in 9:1 of DMSO:Water

Conc. (w/v)	T*gel* (^oC)
0.3	33.9
0.4	42.3
0.5	46.4
0.6	49.1
0.7	52.3
0.8	56.6

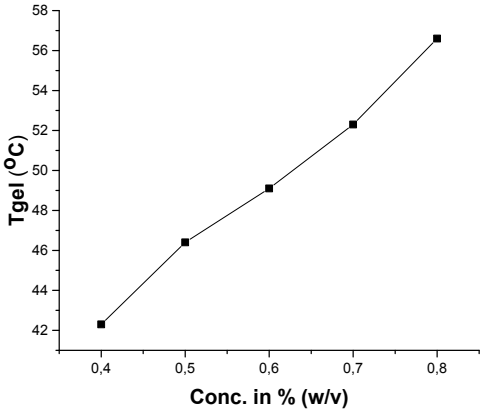

Tgel experiment of 1-$CoCl_2$ gel system against the wt% in 8:2 of DMSO:Water

Conc. (w/v)	T*gel* (^oC)
0.4	41.8
0.5	46.4
0.6	52.8
0.7	55.3
0.8	61

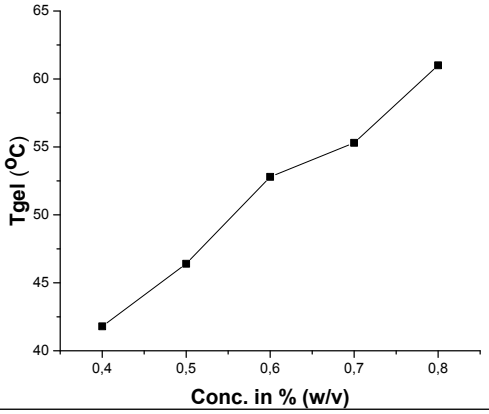

Tgel experiment of 1-$NiCl_2$ gel system against the wt% in 7:3 of DMSO:Water

Conc. (w/v)	T*gel* (^oC)
0.3	58.2
0.4	64.7
0.5	71.1
0.6	77.8
0.7	80.6
0.8	84.4

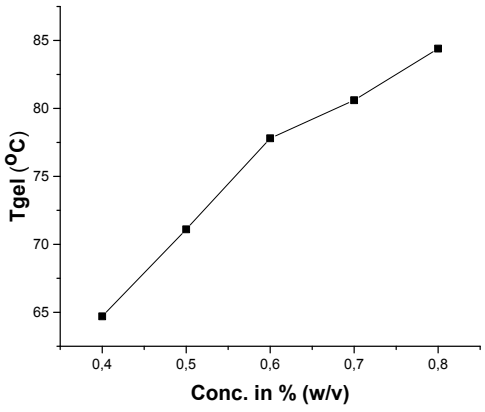

T*gel* experiment of 2-$FeCl_2$ gel system against the wt% in 9:1 of DMSO:Water

Conc. (w/v)	Tgel (°C)
0.4	41.5
0.5	44.6
0.6	47.3
0.7	49.9
0.8	52.6
1	56.6

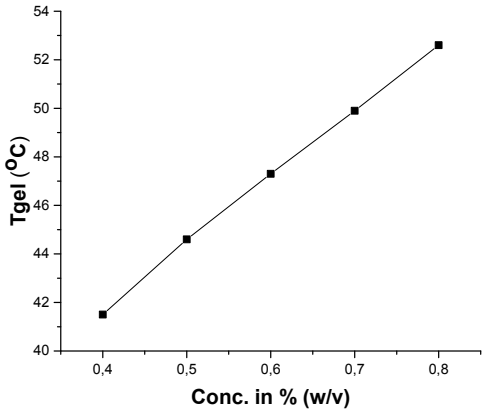

T*gel* experiment of 2-$FeCl_2$ gel system (0.6 % w/v) against the ratio of DMSO:Water.

Ratio of DMSO:Wate	T*gel* (°C)
9.5:0.5	PPt
9:1	48.2
8:2	64.7
7:3	82.1
6:4	98.3
5:5	PPt

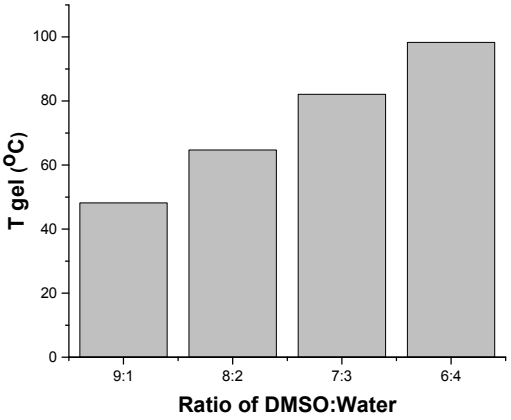

Tgel experiment 2-$FeCl_2$ gel system against the ratio of DMSO:Water.

(0.4 % w/v)			(0.8 % w/v)	
Ratio of DMSO:Water	T*gel* (°C)		Ratio of DMSO:Water	T*gel* (°C)
9.5:0.5	PPt		9.5:0.5	PPt
9:1	41.5		9:1	52.6
8:2	54.3		8:2	76.4
7:3	71.1		7:3	PPt
6:4	86.7		6:4	PPt

T*gel* experiment of 2-$CoCl_2$ gel system against the wt% in 8:2 of DMSO:Water

Conc. (w/v)	T*gel* (°C)
0.3	41.2
0.4	49
0.5	52.6
0.6	56.5
0.7	58.8
0.8	61.4

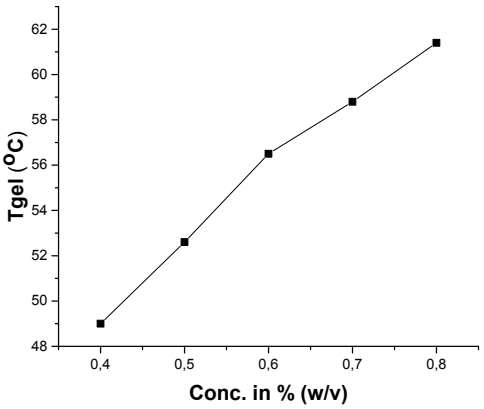

T*gel* experiment of 2-$NiCl_2$ gel system against the wt% in 7:3 of DMSO:Water

Conc. (w/v)	Tgel (°C)
0.3	70.4
0.4	74.3
0.5	79.8
0.6	83.2
0.7	86.1
0.8	90.4

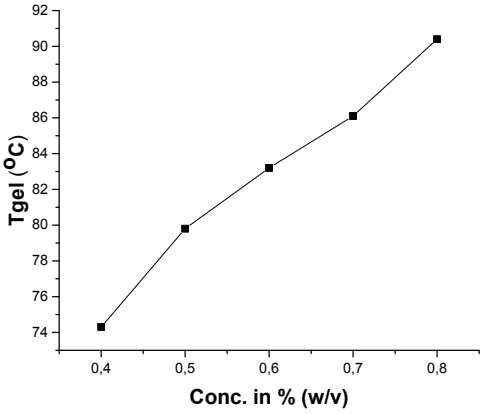

III. Temperature Dependent NMR for 2-$FeCl_2$ system

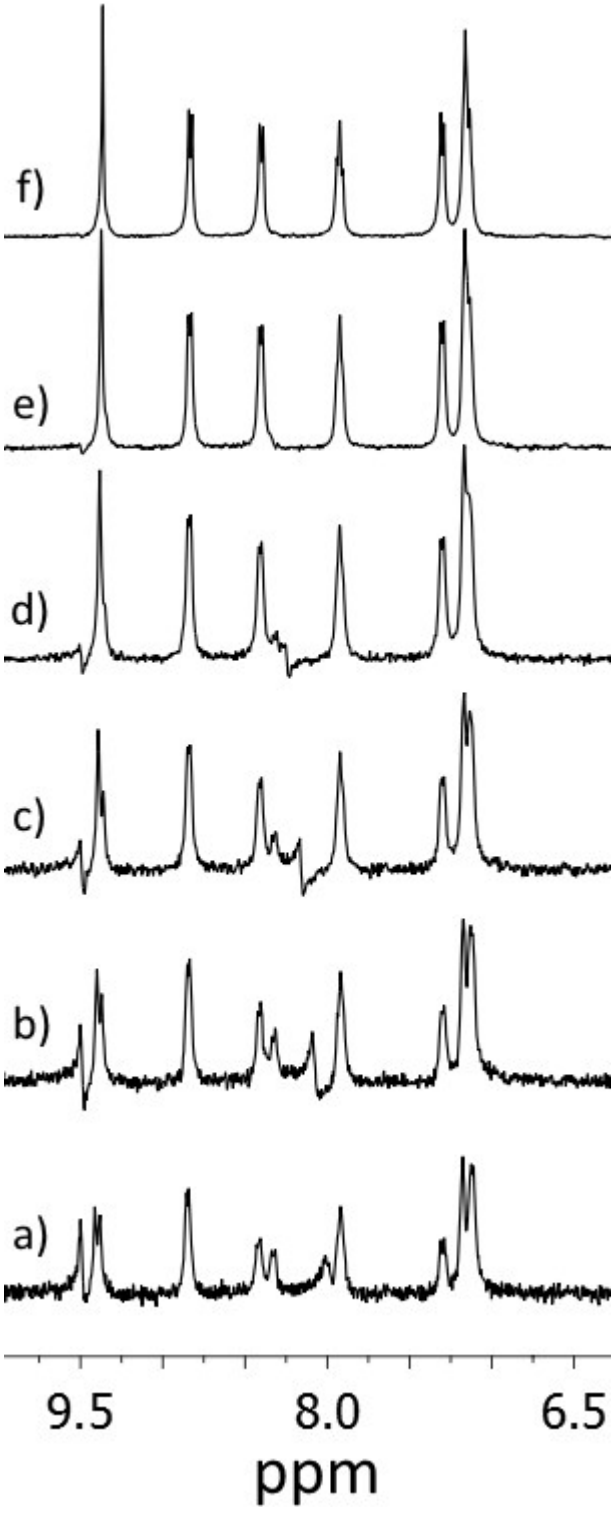

Figure S2. Temperature dependent ^{1}H-NMR spectra of **2**-$FeCl_2$ gel system (from 25 °C to 75°C, 10°C step increase).

IV. Additional SEM and TEM images

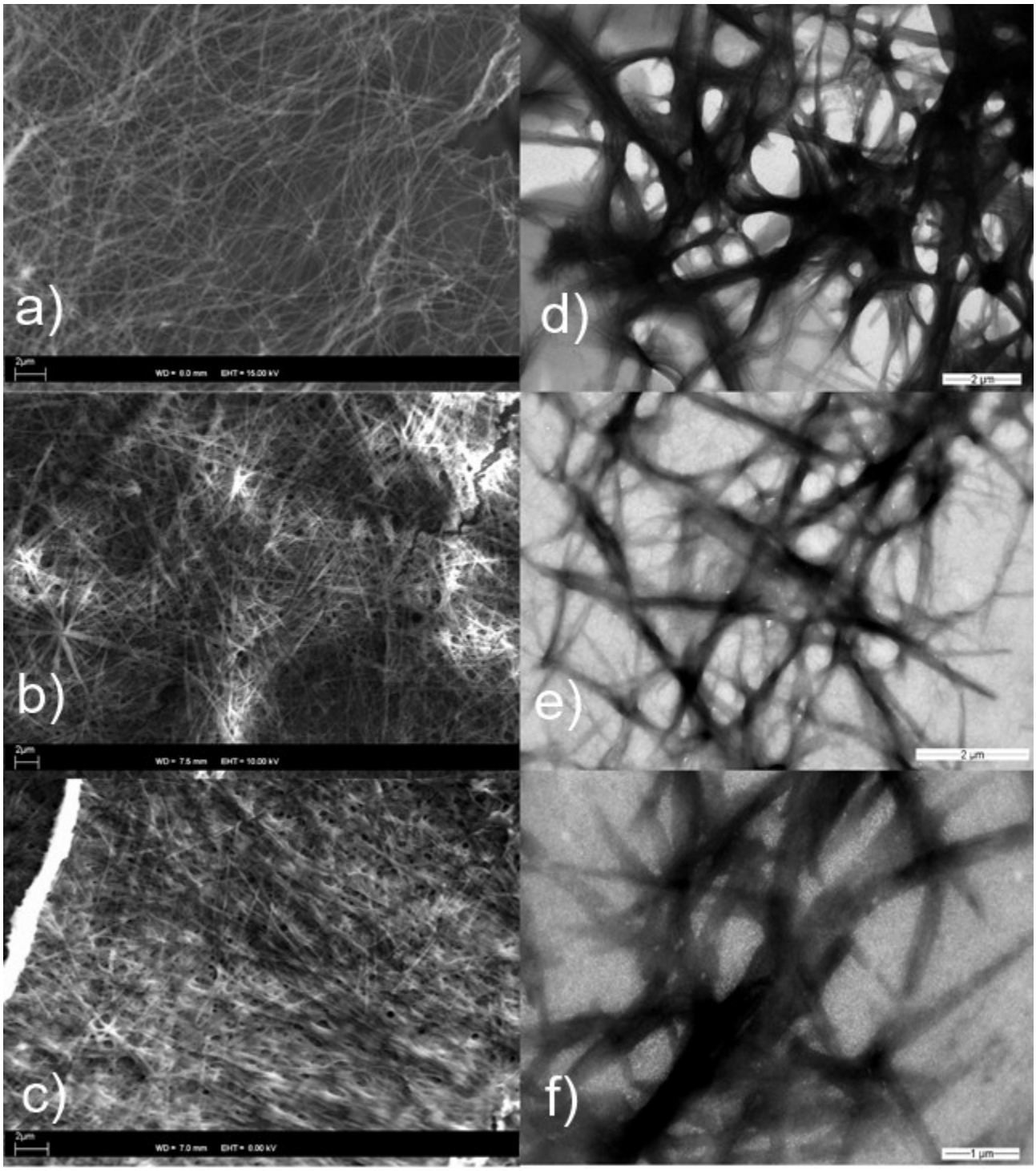

Figure S3. SEM images of metallogels with ligand **2:** a) **2**-$FeCl_2$ in 9:1 DMSO:water mixture; b) **2**-$CoCl_2$ in 8:2 DMSO:water mixture and c) **2**-$NiCl_2$ in 7:3 DMSO:water mixture; and corresponding TEM images d), e) and f), respectively.

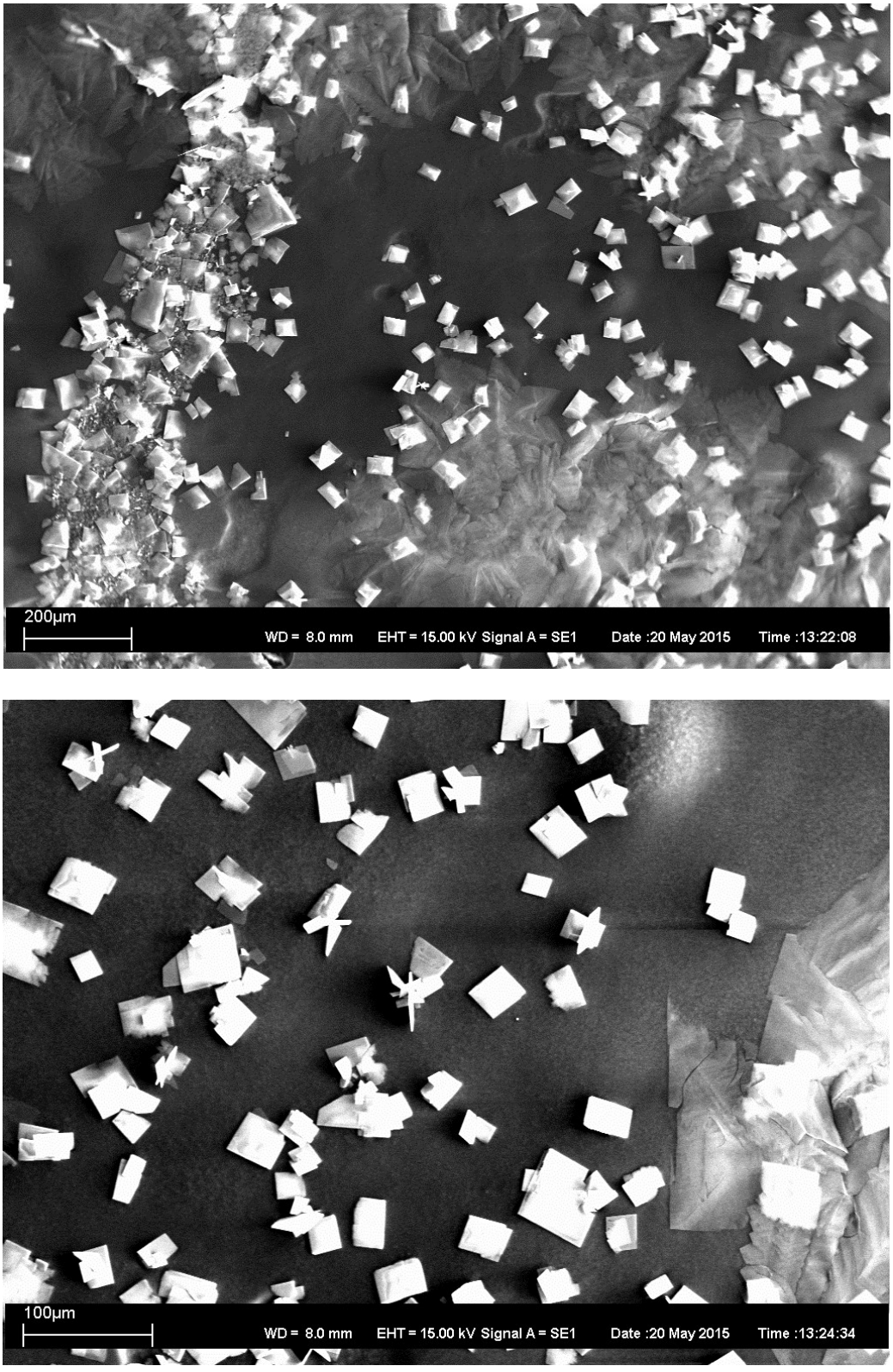

Figure S4. SEM images of the micro-crystalline precipitate made from the disruption of the **1**-$HgCl_2$ gel system.

V. Details on the experiments on the anion effect:

Ligand **1** or **2** was dissolved in 800µl of DMSO and heated to complete solubilization. To this solution 100µl of MCl_2 in water (M = Fe, Co, Zn, or Hg) and 100µl of NaX salt (X = Br^-, AcO^-, NO_3^-, SCN^-, I^- or ClO_3^-, 2 molar equivalents with respect to the MCl_2 to replace both chloride ligands) in water was added and heated to get a clear solution. The solution was then cooled to room temperature and tested about whether it is able to form a gel or not. In the case of $NiCl_2$, ligands were dissolved in 700µl of DMSO and 200µl of $NiCl_2$ and 100µl of NaX salts in water were added.

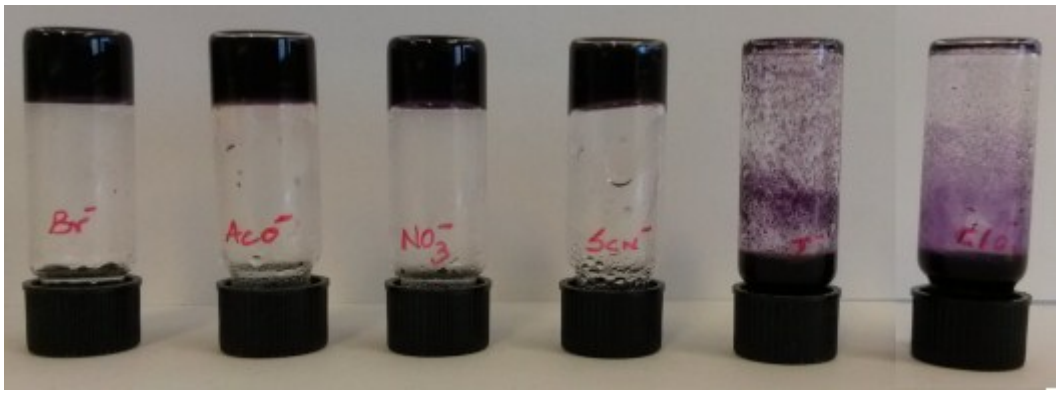

Figure S5. Photographs of the effect of the addition of 2 equivalents of different anionic species to the **2**-$FeCl_2$ gel system.

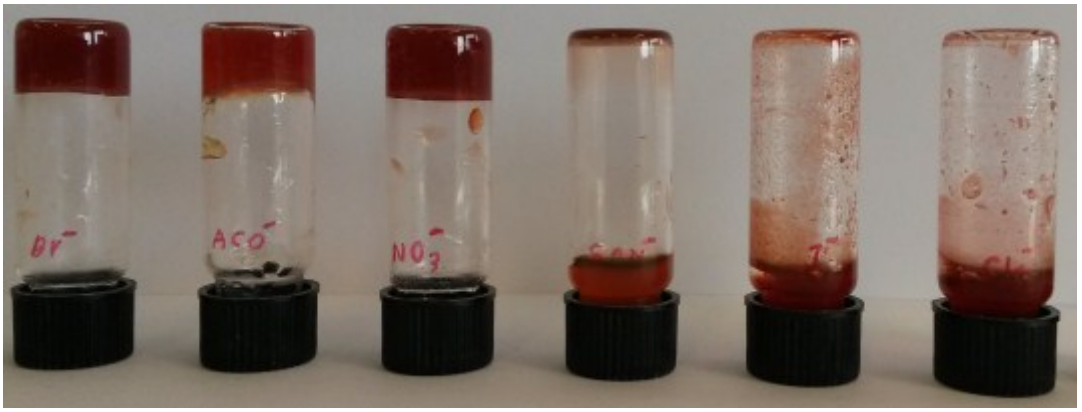

Figure S6. Photographs of the effect of the addition of 2 equivalents of different anionic species to the **2**-$CoCl_2$ gel system.

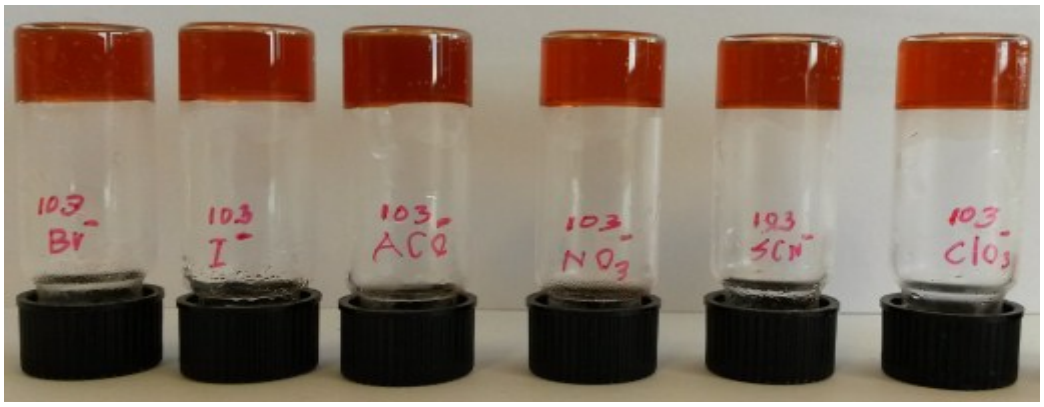

Figure S7. Photographs of the effect of the addition of 2 equivalents of different anionic species to the **1**-$CoCl_2$ gel system.

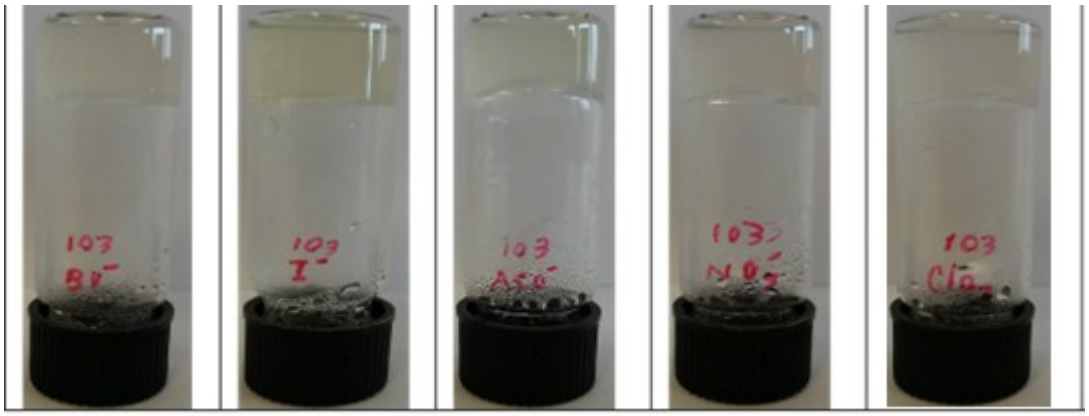

Figure S8. Photographs of the effect of the addition of 2 equivalents of different anionic species to the **1**-$NiCl_2$ gel system.

Effect of addition of increasing amount of chloride ion to the various gel systems:

These experiments also performed in aqueous DMSO solvent (0.8 wt%). The ratio of solvent mixture in Fe, Zn and Hg is 9:1, in cobalt gels with both the ligands are 8:2 and for nickel it is 7:3 due to its gelation conditions.The chloride anion source is tetrabutylammonium chloride TBACl. 1 ml of tetrabutyl ammonium chloride solution was prepared in 9:1 of aqueous DMSO solution for Fe, Zn and Hg. Each 50µl of this solution is two times to the molar amount of MCl_2. For Co and Ni related gels, tetrabutyl ammonium chloride solution was prepared from 8:2 and 7:3 of aqueous DMSO solvents.

Experimental details. 0.8 wt% of the gel was prepared from above refered solvent mixture (9:1, (:2 and 7:3), then the gel was heated to get a clear solution and 50 µl of salt solution was added and cooled to room temperature for obervation. If there is a gel in first addition, then the gel was heated again to have clear solution and then another 50µl of salt solution was added and cooled to room temperature. The procedure was repeated until no gel could be obtained no more.

VI. Temperature Dependent NMR for 2

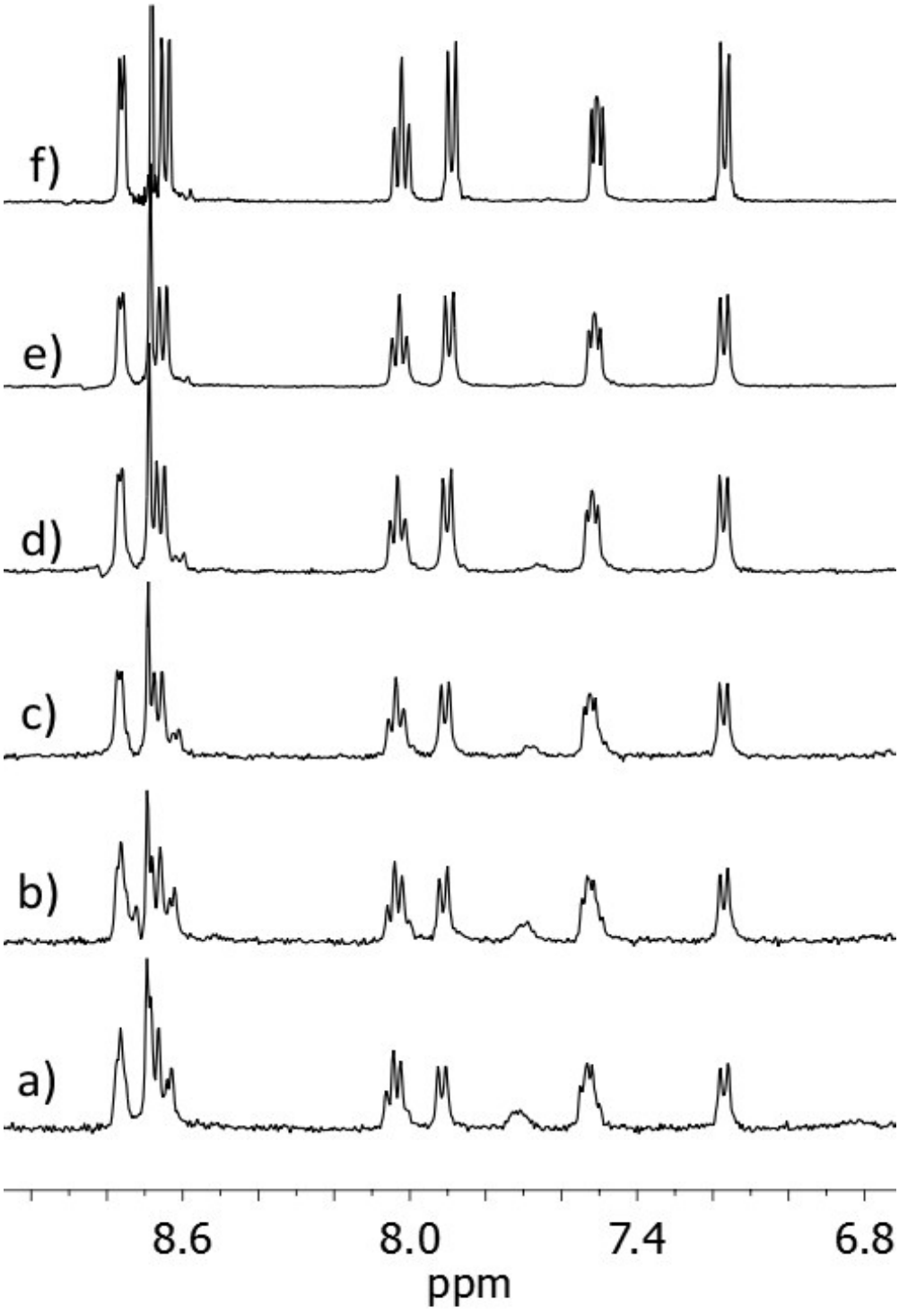

Figure S9. a) Temperature dependent ^{1}H-NMR spectra of ligand **2** (conc. = 1.4 x 10^{-2} M) in DMSO-d_6 from 25° C (a) to 75°C (f) (10 °C step);

VII. Concentration dependent ^{1}H-NMR for 1

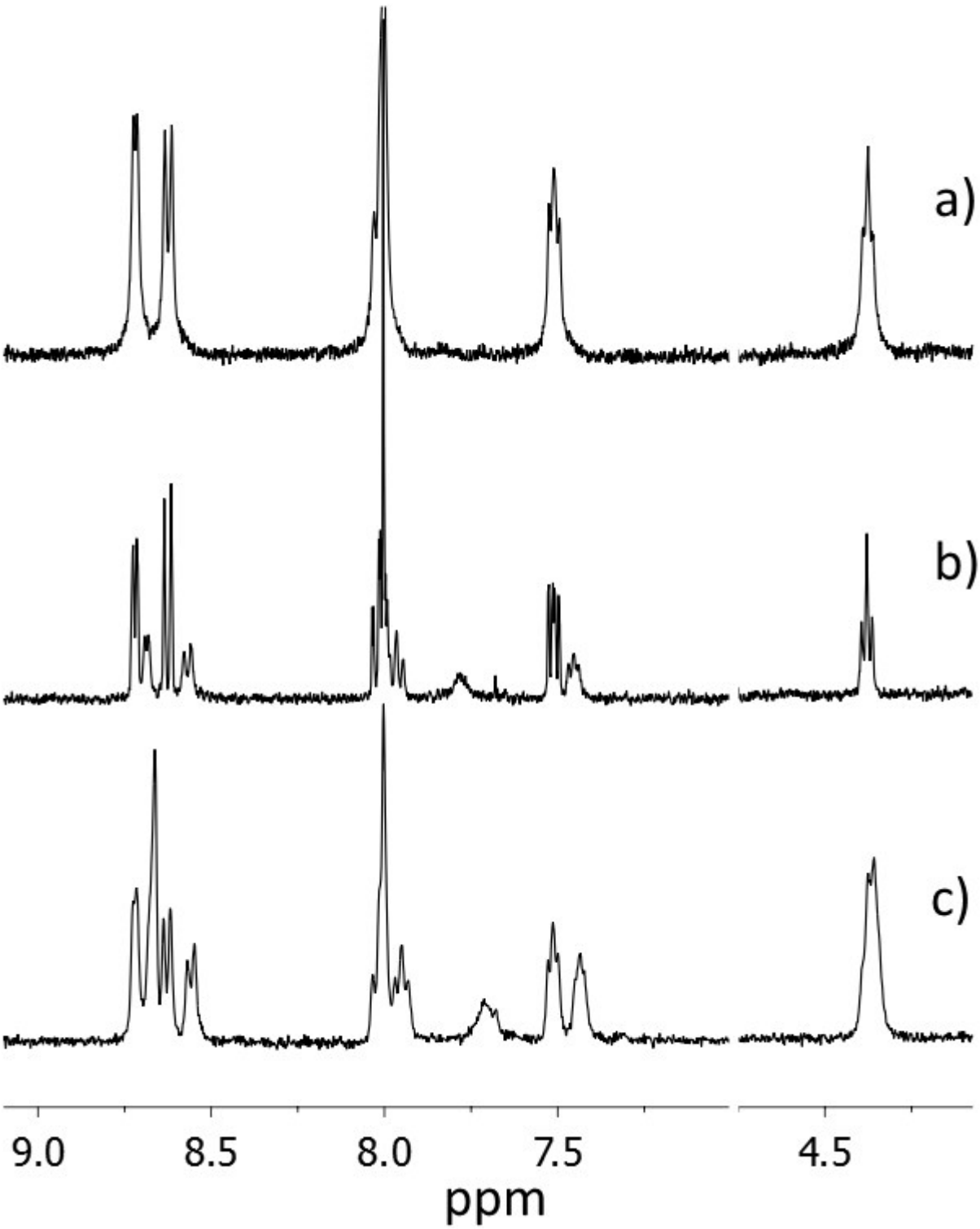

Figure S10. ^{1}H-NMR spectra of ligand **1** in DMSO-d_6 at 25° C and concentrations equal to: a) 4.7 x 10^{-3} M; b) 1.4 x 10^{-2} M, c) 2.3 x 10^{-2} M.

VIII. ^{19}F-NMR data for 1 at different concentrations

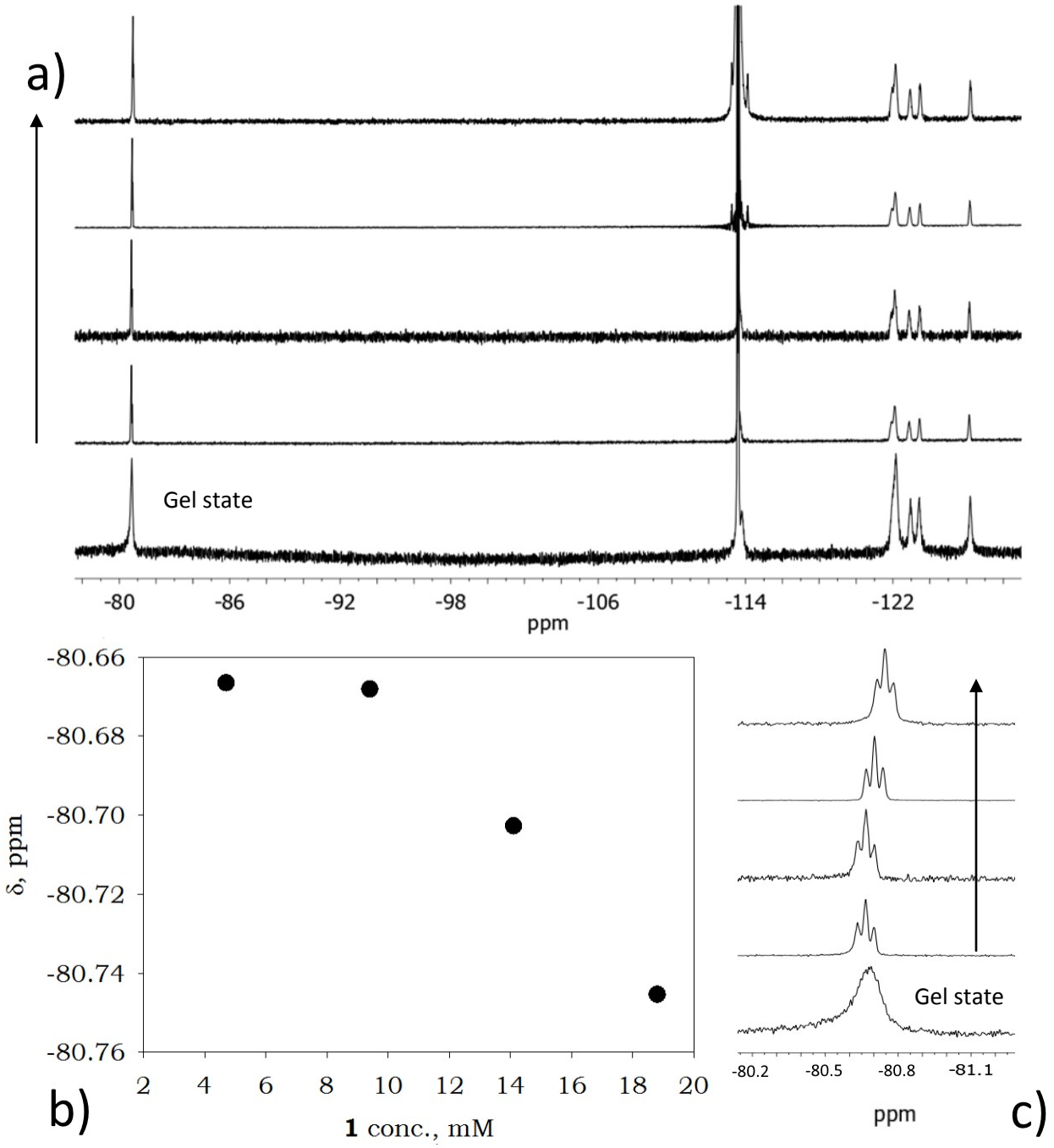

Figure S11. a) ^{19}F-NMR spectra of ligand **1** at various concentrations (from 4.7 x 10^{-3} to 0.0188 M) and in the gel state for **1**-$ZnCl_2$ system; b) Plots of the chemical shift variation upon increasing concentration and c) magnification of the peak centred at ca. -80.5 ppm. Reference C_6H_5F, δ = -113.6 ppm).

IX. Additional Crystallographic Data:

Solid state structure of Ligand **2**:

A)

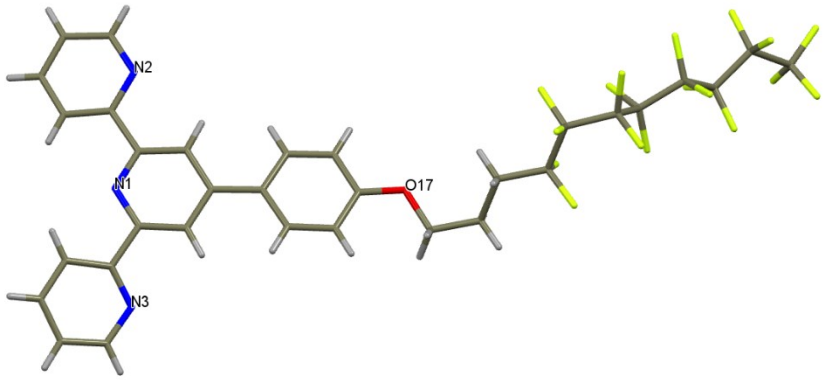

B)

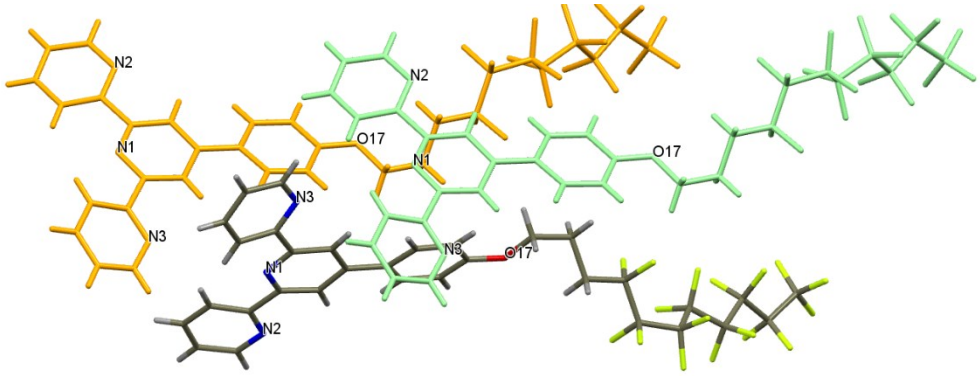

C)

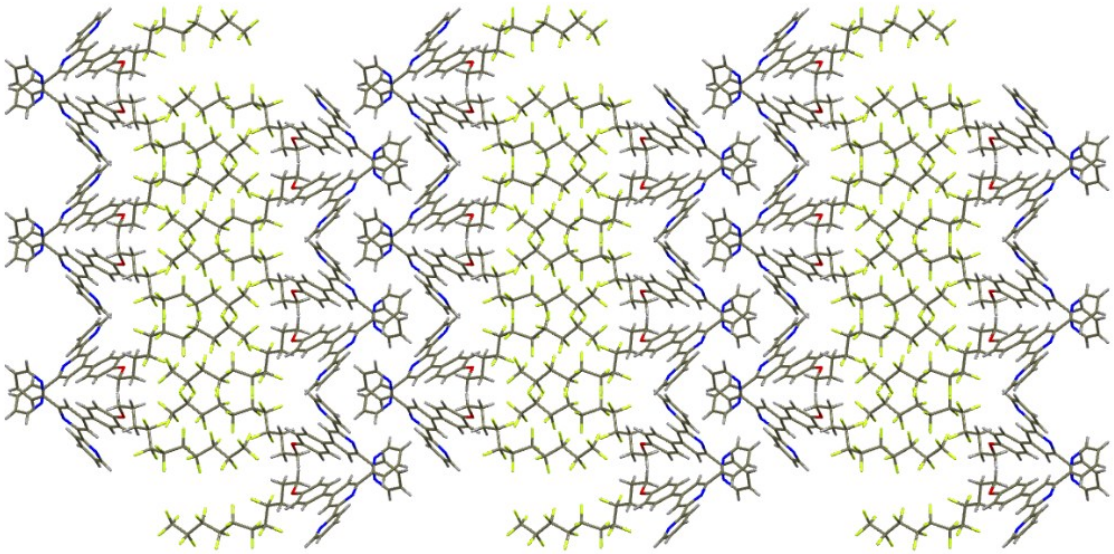

Figure S12. A) X-ray determined structure for ligand **2**: A) molecular structure and B) details of the packing; C) packing.

Table 1: Crystallographic data and structure refinement parameters for the Ligand **2** and for complexes of ligand **1** with Cu, Zn and Hg

	Ligand **2**	**1**-$ZnCl_2$	**1**-$HgCl_2$	**1**-$ZnBr_2$	**1**-$CuCl_2$
CCDC	1477308	1477309	1477310	1477311	1477312
Empirical formula	$C_{32}H_{20}F_{17}N_3O$	$C_{26}H_{16}Cl_2F_{17}N_3OZn$, C_2H_6OS	$C_{26}H_{16}Cl_2F_{17}N_3OHg$, C_2H_3N	$C_{26}H_{16}Br_2F_{17}N_3OZn$, C_2H_6OS	$C_{26}H_{16}Cl_2F_{17}N_3OCu$, C_2H_6OS
Formula weight	785.51	923.81	1021.96	1012.73	921.98
Temp (K)	123	100	120	100	100
Crystal colour, shape	Colorless, Needle	Colorless, Plate	Colorless, Block	Colorless, Block	Blue, Plate
Crystal size/ mm3	0.32 x 0.07 x 0.06	0.11 x 0.07 x 0.04	0.18 x 0.11 x 0.06	0.20 x 0.17 x 0.04	0.08 x 0.06 x 0.02
Crystal system	Monoclinic	Triclinic	Monoclinic	Triclinic	Monoclinic
Space group	$P2_1/c$	$P\bar{1}$	C2/c	$P\bar{1}$	$P2_1/c$
a (Å)	26.1873(11)	7.6578(3)	13.3556(2)	7.66921(15)	27.309(4)
b (Å)	11.4472(4)	10.7944(4)	13.2198(2)	10.9302(2)	12.4387(18)
c (Å)	10.4756(4)	20.9475(10)	38.0862(5)	20.8875(5)	10.4959(13)
α (o)	90	96.942(4)	90	97.0241(17)	90
β (o)	93.328(4)	92.184(4)	97.0770(14)	91.4090(17)	97.544(11)
γ (o)	90	95.173(3)	90	94.9834(16)	90
V (Å3)	3135.0(2)	1709.77(13)	6673.17(17)	1730.10(6)	3534.4(8)
Z	4	2	8	2	4
dcalc (g/cm-3)	1.664	1.794	2.034	1.944	1.733
μ (mm-1)	1.554	1.062	10.942	3.205	0.951
F(000)	1576	920	3920	992	1836
Ref. collected	10952	12136	52501	18565	13287
Ind. reflections	6249	6666	7024	7660	6863
Rint	0.0331	0.0245	0.0728	0.0208	0.0817
GOF	1.050	1.032	1.073	1.051	1.011
R1[a] ($I \geq 2\sigma$)	0.0470	0.0365	0.0543	0.0256	0.0909
wR2[b] ($I \geq 2\sigma$)	0.1231	0.0789	0.1295	0.0595	0.2018

[a] $R1 = \Sigma||F_o| - |F_c||/\Sigma|F_o|$. [b] $wR2 = [\Sigma[w(F_o^2 - F_c^2)^2]/ \Sigma[w(F_o^2)^2]]^{1/2}$.

X. XRPD analysis of 1-$ZnCl_2$ system:

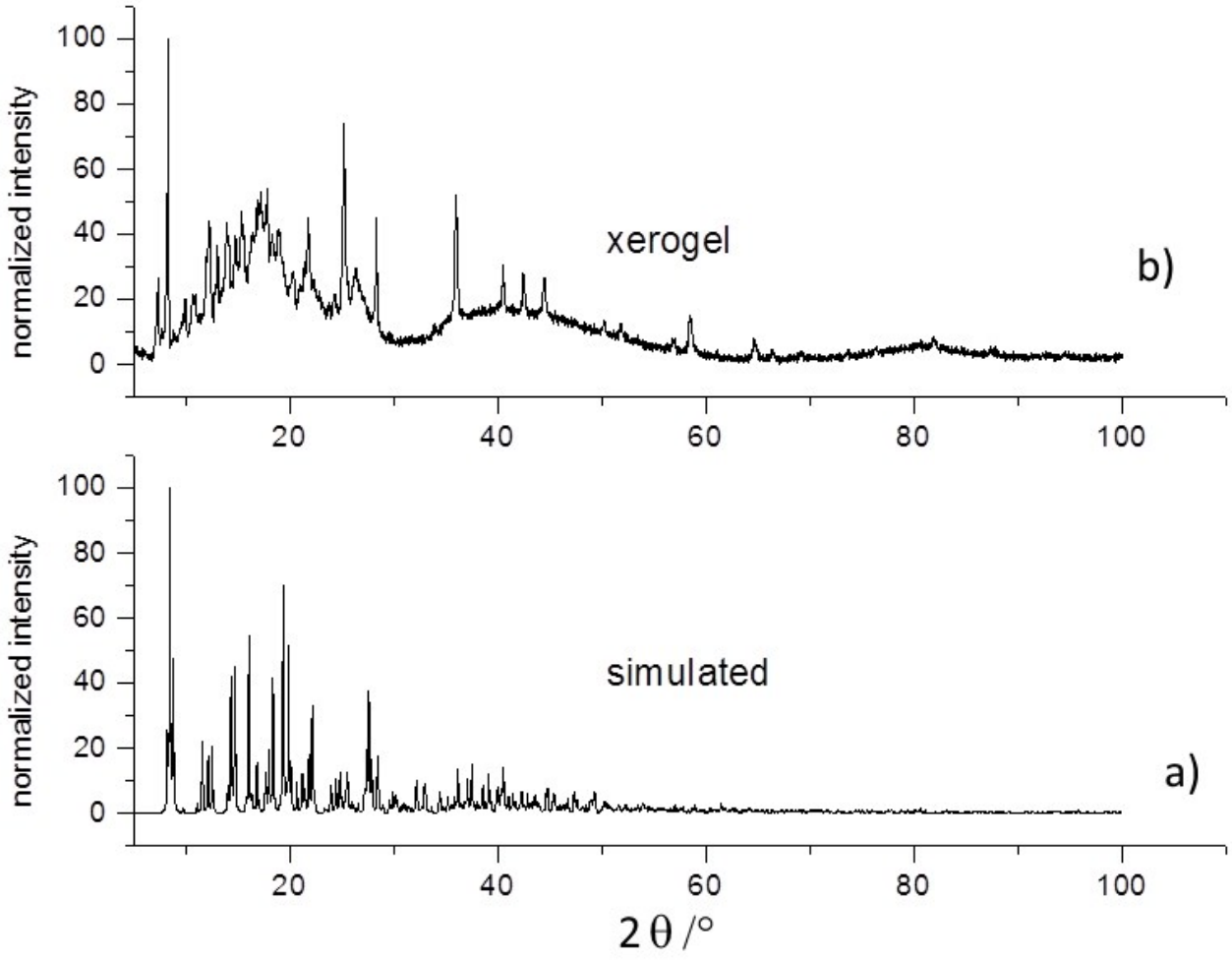

Figure S13. Comparison between the XRPD patterns of **1**-$ZnCl_2$: a) simulated from single crystal X-ray structure, b) xerogel sample